Oxidation of Benzyl Alcohol by a Dioxo Complex of Ruthenium(VI)

Estelle L. Lebeau and Thomas J. Meyer*

Contribution from the Department of Chemistry, CB#3290, Venable Hall, The University of North Carolina, Chapel Hill, North Carolina 27599-3290

Received August 27, 1998

The kinetics and mechanism of reduction of *trans*-$[Ru^{VI}(tpy)(O)_2(L)]^{2+}$ (L is H_2O or CH_3CN; tpy is 2,2′:6′,2″-terpyridine) by benzyl alcohol have been studied in water and acetonitrile. The reactions are first order in alcohol and complex in both solvents and give benzaldehyde as the sole oxidation product. In acetonitrile, sequential $Ru^{VI} \rightarrow Ru^{IV}$ and $Ru^{IV} \rightarrow Ru^{II'}$ steps occur. As shown by FTIR and UV−visible measurements, $Ru^{II'}$ solvolyzes to give $[Ru^{II}(tpy)(CH_3CN)_3]^{2+}$ and benzaldehyde. With ^{18}O-labeled Ru^{VI}, ∼50% of the label ends up in the aldehyde product for both the $Ru^{VI} \rightarrow Ru^{IV}$ and $Ru^{IV} \rightarrow Ru^{II}$ steps as shown by FTIR. In water, $Ru^{VI} \rightarrow Ru^{IV}$ reduction is followed by rapid dimerization by μ-oxo formation. Kinetic parameters for the individual redox steps in 0.1 M $HClO_4$ at 25 °C are $k_{VI\rightarrow IV} = 13.3 \pm 0.8\ M^{-1}\ s^{-1}$ ($\Delta H^{\ddagger} = 11.4 \pm 0.2$ kcal/mol, $\Delta S^{\ddagger} = -15.0 \pm 1$ eu, $k_H/k_D =$ 10.4 for α,α-d_2 benzyl alcohol). In CH_3CN at 25 °C, $k_{VI\rightarrow IV} = 67 \pm 3\ M^{-1}\ s^{-1}$ ($\Delta H^{\ddagger} = 7.5 \pm 0.3$ kcal/mol, $\Delta S^{\ddagger} = -33 \pm 2$ eu, $k_H/k_D = 12.1$) and $k_{IV\rightarrow II'} = 2.4 \pm 0.1$ ($\Delta H^{\ddagger} = 5.1 \pm 0.3$ kcal/mol, $\Delta S^{\ddagger} = -47 \pm 2$ eu, $k_H/k_D =$ 61.5). On the basis of the ^{18}O labeling results in CH_3CN, the O atom of the oxo group transfers to benzyl alcohol in both steps. Mechanisms are proposed involving prior coordination of the alcohol followed by O insertion into a benzylic C−H bond.

Introduction

An extensive library of oxidative reactivity exists for high oxidation state ruthenium-oxo compounds.[1−7] For oxo complexes of Ru(IV), a series of reaction pathways have been identified including epoxidation,[8−12] eletrophilic addition to phenol,[13] and oxidation of alcohols to aldehydes and ketones.[14−22] The oxidation of benzyl alcohol to benzaldehyde by *cis*-$[Ru^{IV}(bpy)_2(py)(O)]^{2+}$ (eq 1) is a significant reaction because of the magnitude of the α,α-CH_2/α,α-CD_2 kinetic isotope effect of $k_H/k_D = 50$ at 25 °C in 0.1 M $HClO_4$.[23] A mechanism has been proposed involving hydride transfer or H atom transfer followed by rapid electron transfer,

$$[Ru^{IV}(bpy)_2(py)(O)]^{2+} + PhCH_2OH \rightarrow [Ru^{II}(bpy)_2(py)(OH)]^{+} + PhCH(OH)^{+} \quad (1a)$$

followed by rapid proton equilibration,

$$[Ru^{II}(bpy)_2(py)(OH)]^{+} + PhCH(OH)^{+} \rightarrow [Ru^{II}(bpy)_2(py)(H_2O)]^{2+} + PhCHO \quad (1b)$$

The reactivity of a family of dioxo complexes of Ru(V) and Ru(VI) is emerging.[3−5,24] This includes the potential 4-electron, dioxo reagent *trans*-$[Ru^{VI}(tpy)(O)_2(S)]^{2+}$, with S = H_2O (**1**-H_2O) or CH_3CN (**1**-CH_3CN).[2,25−28] Previous results have shown that even with the initial *trans*-dioxo geometry, this oxidant is still capable of behaving as a *cis*-dioxo, four-electron oxidant. Mechanistically, this occurs by intramolecular oxo rearrangement following reduction to Ru^{IV}.[29]

In this paper, we describe the kinetics and mechanism of oxidation of benzyl alcohol by **1**. Significant issues that led to

(1) Moyer, B. A.; Sipe, B. K.; Meyer, T. J. *Inorg. Chem.* **1981**, *20*, 1475−1480.
(2) Adeyemi, S. A.; Dovletoglou, A.; Guadalupe, A. R.; Meyer, T. J. *Inorg. Chem.* **1992**, *31*, 1375−1383.
(3) Chronister, C. W.; Binstead, R. A.; Ni, J.; Meyer, T. J. *Inorg. Chem.* **1997**, *37*, 3814−3815.
(4) Che, C.-M., Tang, W.-T.; Wong, W.-T.; Lai, T.-F. *J. Am. Chem. Soc.* **1989**, *111*, 9048.
(5) Groves, J. T.; Quinn, R. *Inorg. Chem.* **1984**, *23*, 3844.
(6) Marmion, M. E.; Takeuchi, K. J. *J. Am. Chem. Soc.* **1988**, *110*, 1472.
(7) Marmion, M. E.; Leising, R. A.; Takeuchi, K. J. *J. Coord. Chem.* **1988**, *19*, 1.
(8) Dobson, J. C.; Seok, W. K.; Meyer, T. J. *Inorg. Chem.* **1986**, *25*, 1514−1516.
(9) Stultz, L. K.; Binstead, R. A.; Reynolds, M. S.; Meyer, T. J. *J. Am. Chem. Soc.* **1995**, *117*, 2520−2532.
(10) Jorgensen, K. A. *Chem. Rev.* **1989**, *89*, 431.
(11) Jorgensen, K. A.; Schiott, B. *Chem. Rev.* **1990**, *90*, 1483.
(12) Khenkin, A. M.; Hill, C. L. *J. Am. Chem. Soc.* **1993**, *115*, 8178.
(13) Seok, W. K.; Meyer, T. J. *J. Am. Chem. Soc.* **1988**, *110*, 7358−7367.
(14) Gerli, A.; Reedijk, J.; Lakin, M. T.; Spek, A. L. *Inorg. Chem.* **1995**, *34*, 1836−1843.
(15) Kutner, W. *J. Electroanal. Chem.* **1989**, *259*, 99−111.
(16) Wong, K.-Y.; Yam, V. W.; Lee, W. W. *Electrochim. Acta* **1992**, *37*, 2645−2650.
(17) Kahn, M. M. T.; Merchant, R. R.; Chatterjee, D.; Bhatt, K. N. *J. Mol. Catal.* **1991**, *67*, 309−315.
(18) Li, C.-K.; Tang, W.-T.; Che, C.-M. Y.; Wong, K.-Y.; Wang, R.-J.; Mak, T. C. W. *J. Chem. Soc., Dalton Trans.* **1991**, 1909−1914.
(19) Wong, K.-Y.; Che, C.-M.; Anson, F. C. *Inorg. Chem.* **1987**, *26*, 737−741.
(20) Marmion, M. E.; Takeuchi, K. J. *J. Chem. Soc., Dalton Trans.* **1988**, 2385−2391.
(21) Che, C.-M.; Ho, C.; Lau, T.-C. *J. Chem. Soc., Dalton Trans.* **1991**, 1901−1907.
(22) Kutner, W.; Gilbert, J. A.; Tomaszewski, A.; Meyer, T. J.; Murray, R. W. *J. Electroanal. Chem.* **1986**, *205*, 185−207.
(23) Roecker, L.; Meyer, T. J. *J. Am. Chem. Soc.* **1987**, *109*, 746−754.
(24) Lebeau, E. L.; Adeyemi, S. A.; Meyer, T. J. *Inorg. Chem.*, **1998**, *37*, 6476−6484.
(25) Dobson, J. C.; Takeuchi, K. J.; Pipes, D. W.; Geselowitz, D. A.; Meyer, T. J. *Inorg. Chem.* **1986**, *25*, 2357.
(26) Che, C.-M.; Lee, W.-O. *J. Chem. Soc., Chem. Commun.* **1988**, 881.
(27) Collin, J. P.; Sauvage, J. P. *Inorg. Chem.* **1986**, *25*, 135.
(28) Goldstein, A. S.; Beer, R. H.; Rheingold, A. L.; Drago, R. S. *J. Am. Chem. Soc.* **1994**, *116*, 2424.
(29) Dovletoglou, A.; Meyer, T. J. *J. Am. Chem. Soc.* **1994**, *116*, 215−223.

10.1021/ic981040v CCC: $18.00
Published on Web 04/17/1999

the study include: (1) How do the mechanistic details compare with those for *cis*-$[Ru^{IV}(bpy)_2(py)(O)]^{2+}$ and related oxidants? What are the differences, if any, between Ru^{VI} and Ru^{IV} as oxidants? (2) Are there special pathways that appear associated with the four-electron acceptor ability of **1**. (3) How do k_H/k_D kinetic isotope effects compare for Ru^{VI} compared to Ru^{IV}?

Experimental Section

Materials. High-purity acetonitrile (Burdick & Jackson) was used as the solvent for kinetic studies after distillation from P_2O_5 with use of a Vigereux column. High-quality deionized water ($\geq$16.5 MΩ) was prepared by passing house-distilled water through a Nanopure (Barnstead) water purification system. High-purity NMR solvents, ^{18}O-labeled $H_2{}^{18}O$ (Cambridge Isotope Laboratories), α,α-d_2-benzyl alcohol (99.8%, Isotec, Inc, Miamisburg, OH), deuterium oxide, and doubly distilled perchloric acid (G. Frederick Smith) were used as received without additional purification. High-purity (99.9%) benzyl alcohol was obtained from Aldrich. Purity was verified by silica TLC (80:20, hexanes/ethyl acetate) and ^1H NMR. All other common reagents were ACS grade and used without additional purification.

Preparations. *trans*-$[Ru^{VI}(tpy)(O)_2(H_2O)](ClO_4)_2$ was prepared by using a literature method.[2] ***Caution!*** *Particular care should be exercised in the preparation and handling of transition metal perchlorate salts. This salt is known to explode spontaneously and violently when dried extensively*.

***trans*-$[Ru^{VI}(tpy)(^{18}O)_2(H_2{}^{18}O)](ClO_4)_2$.** A 50 mg (0.11-mmol) quantity of $[Ru^{II}(tpy)(C_2O_4)(H_2O)]\cdot 2H_2O$ was suspended and stirred for 1 h in 1 mL of a 2 M $HClO_4$ solution which was prepared by using ^{18}O-labeled water. This solution was added dropwise to a magnetically stirred solution containing a 20-fold excess of Ce^{IV} (as $[(NH_4)_2Ce^{IV}(NO_3)_6]$ in 2 M $HClO_4$ made in ^{18}O-labeled water). The reaction mixture was cooled for $\sim$2 h at 0 °C. A yellow solid appeared and was collected by centrifugation followed by decanting of the supernatant. ^{18}O label incorporation was determined to be $\sim$72% in CH_3CN by FTIR analysis of the symmetric and asymmetric modes for the *trans*-dioxo group.[30]

Instrumentation. UV−visible kinetic measurements for rapid reactions were made by use of a Hi-Tech CU-61 rapid scanning spectrophotometer attached to a Hi-Tech Scientific SF-61 double mixing stopped-flow apparatus by using the KinetAsyst 2.0 software program. For slower reactions, spectra were obtained as a function of time by use of a Hewlett-Packard 8452A diode array spectrophotometer. Manual mixing of solutions from conventional syringes into standard cuvettes was employed. Kinetic runs were initiated by mixing an equivalent volume of alcohol solution with the ruthenium solution. Substrate concentrations were calculated from known molar absorptivities of the Ru^{VI} species and from the known densities of the liquid alcohols. The temperatures of solutions during kinetic studies was maintained to within ±0.2 °C with use of a Lauda RM6 or a Neslab RTE-110 circulating water baths and monitored with an Omega HH-51 thermocouple probe. ^1H NMR spectra were obtained in D_2O or CD_3CN by using Bruker WM-250 MHz FT-NMR or AC-200 MHz FT-NMR spectrometers. Reaction mixtures were analyzed by use of a Hewlett-Packard 5890 Series II gas chromatograph with a 12 m × 0.2 mm × 0.33 μm HP-1 column and a Hewlett-Packard 5971A mass selective detector. IR spectra were recorded on a Mattson Galaxy 5020 series FTIR spectrophotometer with a liquid nitrogen cooled external detector by Gaseby Infrared (model MI 0465-0052-6) and had 2 cm^{-1} resolution. IR measurements were made in CD_3CN solution by use of a demountable cell with NaCl plates and Teflon spacers or a fused BaF_2 cell with a 1 mm path length. Unless otherwise noted, experiments were performed under aerobic conditions.

Kinetics. Spectral-kinetic data were processed by use of either the program KINFIT[31] or SPECFIT.[32] Use of SPECFIT gives the predicted spectra of the colored species, concentration profiles with time, and globally optimized rate constants. Each reported rate constant is the average of 8−15 separate experimental determinations performed under constant reaction conditions.

Results

Product Analysis and Stoichiometry. H_2O. Kinetic data for oxidations involving *trans*-$[Ru^{VI}(tpy)(O)_2(H_2O)]^{2+}$ in 0.1 M $HClO_4$ were obtained from absorbance-time traces from $\sim$350 to 700 nm. A typical trace is shown in Figure 1 of the Supporting Information. At early times (<300 s), $[Ru^{VI}(tpy)(O)_2(H_2O)]^{2+}$ (λ_{max} = 410 nm, ϵ = 3700 M^{-1} cm^{-1})[2] disappears with simultaneous growth of a new spectral feature near 440 nm. This spectrum evolves into a complicated spectrum which includes an absorption at >650 nm, indicative of higher oligomers.[24] Reduction of **1**-H_2O to Ru^{IV} by Fe^{II} or hydroquinone gives $[(tpy)(H_2O)_2Ru^{IV}ORu^{IV}(H_2O)(OH)(tpy)]^{5+}$ followed by slower reduction to $[(tpy)(H_2O)_2Ru^{III}ORu^{IV}(H_2O)(OH)(tpy)]^{4+}$ and $[(tpy)(H_2O)_2Ru^{III}ORu^{III}(H_2O)_2(tpy)]^{4+}$.[24]

Product studies by GC−MS (following CH_2Cl_2 extraction) show that at a 1:1 ratio of benzyl alcohol to *trans*-$[Ru^{VI}(tpy)(O)_2(H_2O)]^{2+}$, the sole product in stoichiometric or near-stoichiometric amounts is benzaldehyde consistent with,

$$2\ \textit{trans}\text{-}[Ru^{VI}(tpy)(O)_2(H_2O)]^{2+} + 2\ PhCH_2OH \rightarrow [(tpy)(H_2O)_2Ru^{IV}ORu^{IV}(OH)(H_2O)(tpy)]^{5+} + 2\ PhCHO \quad (2)$$

Independent experiments show that the $Ru^{III}ORu^{IV}$ and $Ru^{IV}ORu^{IV}$ forms of the μ-oxo dimer do oxidize benzyl alcohol to benzaldehyde in 0.1 M $HClO_4$ but on a longer time scale than for the mixing experiments in Figure 1 of the Supporting Information. With excess benzyl alcohol, the ultimate product is $[Ru^{II}(tpy)(H_2O)_3]^{2+}$ (λ_{max} = 532 nm, ϵ = 3450 M^{-1} cm^{-1}).[2] These reactions presumably occur by one-electron pathways and intermediate radical formation.[33] Under anaerobic conditions, with $Ru^{IV}ORu^{IV}$ as oxidant, the stoichiometry is

$$[(tpy)(H_2O)_2Ru^{IV}ORu^{IV}(OH)(H_2O)(tpy)]^{5+} + PhCH_2OH \rightarrow [(tpy)(H_2O)_2Ru^{III}ORu^{III}(H_2O)_2(tpy)]^{4+} + PhCHO \quad (3)$$

Product Analysis and Stoichiometry. Acetonitrile. In Figure 1 are shown visible spectral changes with time for the reaction between *trans*-$[Ru^{VI}(tpy)(O)_2(CH_3CN)]^{2+}$ (1.6×10^{-4} M) and benzyl alcohol (1.6×10^{-3} M) in CH_3CN at 25 °C. A sequence of reactions occurs, but there is no sign of dimerization or higher oligomerization. In stage 1 (<60 s) Ru^{VI} (λ_{max} = 416 nm, ϵ = 3500 cm^{-1} M^{-1}) is lost concomitant with appearance of a broad, new spectral feature at lower energy. In stage 2, this feature evolves nearly isosbestically into a spectrum similar to that of $[Ru^{II}(tpy)(CH_3CN)_3]^{2+}$, but with a shoulder that extends into the low-energy visible range. In stage 3, the spectrum further evolves into $[Ru^{II}(tpy)(CH_3CN)_3]^{2+}$ with λ_{max} values at 419 and 435 nm.[34]

The reaction with benzyl alcohol was also investigated by FTIR in the region 1750−1300 cm^{-1} (Figure 2 of the Supporting Information). Even with fast mixing, stages 1 and 2 were complete by the first scan, acquired <10 s after mixing. New bands appear in the initial spectrum at 1702 {ν(C=O), benzaldehyde}, 1479, and 1318 cm^{-1}. At the first scan, 1 equiv of

(30) Dovletoglou, A. Ph.D. Dissertation, University of North Carolina, Chapel Hill, NC, 1992.
(31) Binstead, R. A. *KINFIT Nonlinear Curve Fitting for Kinetic Systems*; Chemistry Department, University of North Carolina: Chapel Hill, NC, 1990.
(32) Spectrum Software Associates, Chapel Hill, NC.
(33) Lebeau, E. L. Ph.D. Dissertation, University of North Carolina, Chapel Hill, NC, 1997.
(34) Suen, H.-F.; Wilson, S. W.; Pomerantz, M.; Walsh, J. L. *Inorg. Chem.* **1989**, *28*, 786−791.

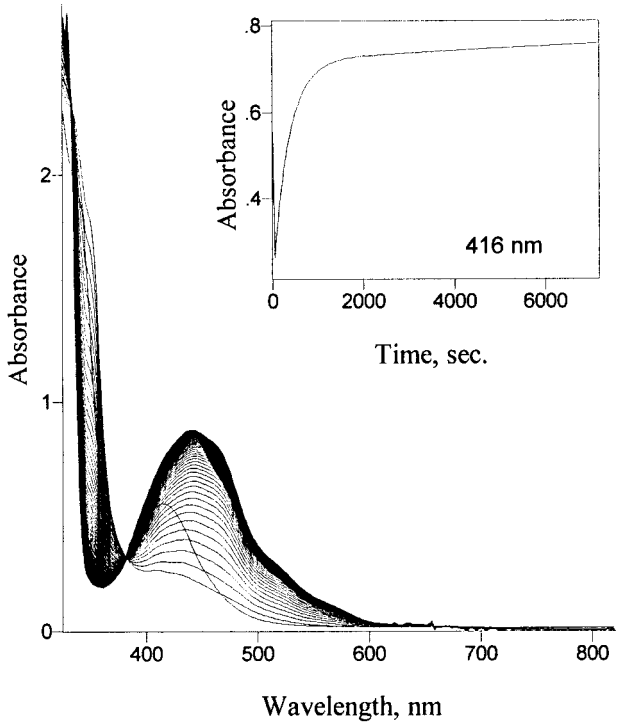

Figure 1. Absorbance-time traces at various intervals over a period of 2 h for the reaction between *trans*-$[Ru^{VI}(tpy)(O)_2(CH_3CN)]^{2+}$ (1.6×10^{-4} M) and benzyl alcohol (1.6×10^{-3} M) in CH_3CN at 25 °C. Inset shows absorbance changes with time at 416 nm which is a λ_{max} for *trans*-$[Ru^{VI}(tpy)(O)_2(CH_3CN)]^{2+}$.

benzaldehyde (compared to the initial *trans*-$[Ru^{VI}(tpy)(O)_2(CH_3CN)]^{2+}$) had appeared based on the integrated intensity of ν(C═O) as determined by a calibration curve. All other bands in the spectrum are assignable to solvent, benzyl alcohol, or benzaldehyde.

The new bands at 1479 and 1318 cm^{-1} disappear at the same rate as an additional increase in ν(C═O). On the basis of the results of parallel experiments with UV−visible monitoring, this process occurs on the same time scale as stage 3, in which solvolysis occurs to give free benzaldehyde and $[Ru^{II}(tpy)(CH_3CN)_3]^{2+}$. The additional benzaldehyde produced at this stage is equal to the amount produced in the first stage by IR. The net stoichiometry based on FTIR, UV−visible, and ^1H NMR analysis is

$$trans\text{-}[Ru^{VI}(tpy)(O)_2(CH_3CN)]^{2+} + 2\ PhCH_2OH \rightarrow [Ru^{II}(tpy)(CH_3CN)_3]^{2+} + 2\ PhCHO \quad (4)$$

The same stoichiometry was obtained with 1:2 to 1:10 ratios of $[Ru^{VI}(tpy)(O)_2(CH_3CN)]^{2+}$/benzyl alcohol based on IR peak height measurements. At a 1:1 ratio, ν(C═O) for benzoic acid at 1725 cm^{-1} appears, but only after several hours.

The FTIR experiment was repeated with 72% ^{18}O-labeled *trans*-$[Ru^{VI}(tpy)(O)_2(CH_3CN)]^{2+}$. After the labeled complex was mixed in a 1:4 ratio with benzyl alcohol, band intensities at both ν(C═O) and ν(C═^{18}O) (at 1657 cm^{-1}) were measured. Based on the calibration curve ~30(±5)% of the benzaldehyde present initially was ^{18}O labeled. Following the second, time-resolved step, the extent of incorporation was ~34(±5)%. These results are consistent with incorporation of ~50% of the label originally in *trans*-$[Ru^{VI}(tpy)(^{18}O)_2(CH_3CN)]^{2+}$) into the benzaldehyde product at each step.

Product Analysis and Stoichiometry. CH_3CN/H_2O Mixtures. In acetonitrile, 2.85 M in added water, the equilibrium

Table 1. Kinetic Parameters for $PhCH_2OH$ (and $PhCD_2OH$) Oxidation by *trans*-$[Ru^{VI}(tpy)(O)_2(L)]^{2+}$ (L = H_2O, D_2O, CH_3CN) and Ru^{IV} at 25 °C

L	k (M^{-1} s^{-1})	solvent	$\Delta H^{\ddagger}$ (kcal/mol)	$\Delta S^{\ddagger}$ (eu)	k_H/k_D
		Oxidation by Ru^{VI}			
H_2O	13.3 ± 0.8	0.1 M $HClO_4$	11.4 ± 0.2	−15.0 ± 1	10.4 ± 0.8
H_2O[a]	1.3 ± 0.2	0.1 M $HClO_4$	14.0 ± 0.2	−10.8 ± 1	
D_2O	12.8 ± 0.3	0.1 M $HClO_4$			
H_2O[b]	28 ± 4	CH_3CN			
CH_3CN	62 ± 3	CH_3CN	7.5 ± 0.4	−33 ± 2	12.1 ± 0.7
CH_3CN[a]	5.5 ± 0.3	CH_3CN	8.6 ± 0.4	−34 ± 2	
		Oxidation by Ru^{IV}			
CH_3CN	2.4 ± 0.1	CH_3CN	5.1 ± 0.3	−47 ± 2	
CH_3CN[a]	$3.9 \pm 0.2 \times 10^{-2}$	CH_3CN	9.9 ± 0.5	−39 ± 2	61.5 ± 1.2

[a] Oxidation of α,α-d_2 benzyl alcohol. [b] In CH_3CN, 2.85 M in H_2O.

$$trans\text{-}[Ru^{VI}(tpy)(O)_2(H_2O)]^{2+} + CH_3CN \underset{k_r}{\overset{k_f}{\rightleftharpoons}} trans\text{-}[Ru^{VI}(tpy)(O)_2(CH_3CN)]^{2+} + H_2O \quad (5)$$

lies 95% toward *trans*-$[Ru^{VI}(tpy)(O)_2(H_2O)]^{2+}$ ($K = 0.15$).[2] Under these conditions, the spectral changes observed upon addition of $PhCH_2OH$ are essentially those in Figure 1 of the Supporting Information. Ru^{VI} reduction to Ru^{IV} is followed by rapid μ-oxo formation.

Reduction of *trans*-$[Ru^{VI}(tpy)(O)_2(CH_3CN)]^{2+}$ with hydroquinone in dry CH_3CN also occurs with μ-oxo formation to give $Ru^{IV}ORu^{IV}$ as the initial product. It is reduced further to $Ru^{III}ORu^{III}$. Addition of an excess of ascorbic acid results in quantitative formation of $[Ru^{II}(tpy)(CH_3CN)_3]^{2+}$.

All attempts, chemical and electrochemical, to generate $[Ru^{IV}(tpy)(CH_3CN)_2(O)]^{2+}$ independently were unsuccessful due to dimer formation. Kinetics studies of benzyl alcohol oxidation by Ru^{IV} were followed as the second stage in the net reduction of Ru^{VI} to $[Ru^{II}(tpy)(CH_3CN)_3]^{2+}$.

Kinetics and Mechanism. Water. From concentration dependence studies in the kinetics of Ru^{VI} reduction by $PhCH_2OH$, loss of Ru^{VI} is first order in both Ru^{VI} and benzyl alcohol. A plot of k_{obs} versus alcohol concentration was linear from $[PhCH_2OH] = 5.0 \times 10^{-1}$ to 5.0×10^{-4} M with $[Ru^{VI}] = 5.0 \times 10^{-5}$ M (Figure 5 of the Supporting Information). The quantitative evaluation of k_{obs} involved fitting over 80 separate kinetic runs which included an average of 9−13 experimental determinations under each set of reaction conditions. The results are consistent with the rate law,

$$-d[Ru^{VI}]/dt = k_{obs}[Ru^{VI}][\text{benzyl alcohol}] \quad (6)$$

Rate constants are listed in Table 1. These data include the reaction with α,α-d_2 benzyl alcohol for which an α,α-CD_2 kinetic isotope effect of $k_H/k_D = 10.4$ can be calculated. The solvent kinetic isotope effect is small ($k_{H_2O}/k_{D_2O} = 1.04$).

Temperature dependence studies were conducted between 5.0 and 50.0 °C. Plots of $\ln(k_{obs}/T)$ versus $1/T$ were linear (Figure 4 of the Supporting Information) as predicted by the Eyring equation (eq 7). The data are listed in Table 1.

$$k_{obs} = (k_B T/h) \exp(-\Delta G^{\ddagger}/RT) = (k_B T/h) \exp(-\Delta H^{\ddagger}/RT) \exp(\Delta S^{\ddagger}/R) \quad (7)$$

Acetonitrile. Stage 1. In stage 1, Ru^{VI} is reduced to Ru^{IV}. With benzyl alcohol in pseudo-first-order excess over *trans*-$[Ru^{VI}(tpy)(O)_2(CH_3CN)]^{2+}$, the first stage is kinetically separable

from the following reactions. From measurements between 325 and 820 nm, with [benzyl alcohol] from 1.51×10^{-4} to 1.51×10^{-2} M, a plot of k_{obs} vs [$PhCH_2OH$] was linear, consistent with the rate law

$$-d[Ru^{VI}]/dt = k_1[Ru^{VI}][PhCH_2OH] \quad (8)$$

From the slope of the plot, $k_1 = 67(\pm 3)$ M^{-1} s^{-1} at 25 °C. With α,α-d_2 benzyl alcohol as reductant, $k_1 = 5.5(\pm 0.3)$ M^{-1} s^{-1}, and $k_H/k_D = 12.1$. The kinetics of both reactions were investigated from 5 to 47.5 °C, and activation parameters are listed in Table 1.

Stage 2. In stage 2, Ru^{IV} is reduced to a Ru^{II} intermediate, $Ru^{II'}$. It is kinetically separable from the other two stages. From kinetic studies over the range [$PhCH_2OH$] $= 1.5 \times 10^{-2}$ to 1.5×10^{-4} M, k_2 varies linearly with [$PhCH_2OH$] consistent with the rate law

$$-d[Ru^{IV}]/dt = k_2[Ru^{IV}][PhCH_2OH] \quad (9)$$

with k_2 (25 °C) $= 2.4(\pm 0.01)$ M^{-1} s^{-1} and k_2 (25 °C) $= 3.9(\pm 0.02) \times 10^{-2}$ M^{-1} s^{-1} for reaction with α,α-d_2 benzyl alcohol, Table 1. Activation parameters are listed in Table 1.

Stage 3. In stage 3, $Ru^{II'}$ undergoes solvolysis to give $[Ru^{II}(tpy)(CH_3CN)_3]^{2+}$ (as shown by UV−visible measurements) and benzaldehyde (by FTIR). The kinetics are first order, consistent with the rate law

$$-d[Ru^{II'}]/dt = k_3[Ru^{II'}] \quad (10)$$

with k_3 (25 °C) $= 1.13(\pm 0.06) \times 10^{-4}$ s^{-1}. For comparison, under the same conditions, substitution of CH_3CN for H_2O in *cis*-$[Ru^{II}(bpy)_2(py)(H_2O)]^{2+}$ occurs with k (25 °C) $= 1.66(\pm 0.02) \times 10^{-3}$ s^{-1}.[35]

Global Kinetic Analysis in Acetonitrile. As a further confirmation of mechanism, absorbance−time data monitored from ~300 to 750 nm under conditions where the three stages were kinetically coupled, were analyzed by applying a global kinetic analysis based on the reactions in Scheme 1. Singular value decomposition (SVD) of the data shown in Figure 1 revealed the presence of four significant time (**U** × **S**) and spectral domain eigenvectors (**V**).[36] Additional eigenvectors contained only lamp and random noise which was factored out of the data. The presence of four significant eigenvectors implies a *minimum* of three distinct kinetic processes.

The data were fit to the mechanism in Scheme 1 by using the program SPECFIT.[32b,36] It uses a stiff differential numerical integration method and fits the data globally. Predicted spectra are shown in Figure 2, and rate constants are shown in Scheme 1. Spectra for *trans*-$[Ru^{VI}(tpy)(O)_2(CH_3CN)]^{2+}$ and $[Ru^{II}(tpy)(CH_3CN)_3]^{2+}$ compare well with known spectra as do the rate constants with those obtained by kinetic isolation (Table 1). (In a previous publication,[2] the spectrum claimed to be Ru^{IV} is actually that of Ru^{III}.) Examples of single-wavelength absorbance−time traces, fits, and residuals are shown in Figure 3. Several different models were examined when fitting the data. Only the model presented in Scheme 1 returned both satisfactory fits to the data as well as acceptable predicted spectra that compared well to the known spectra.

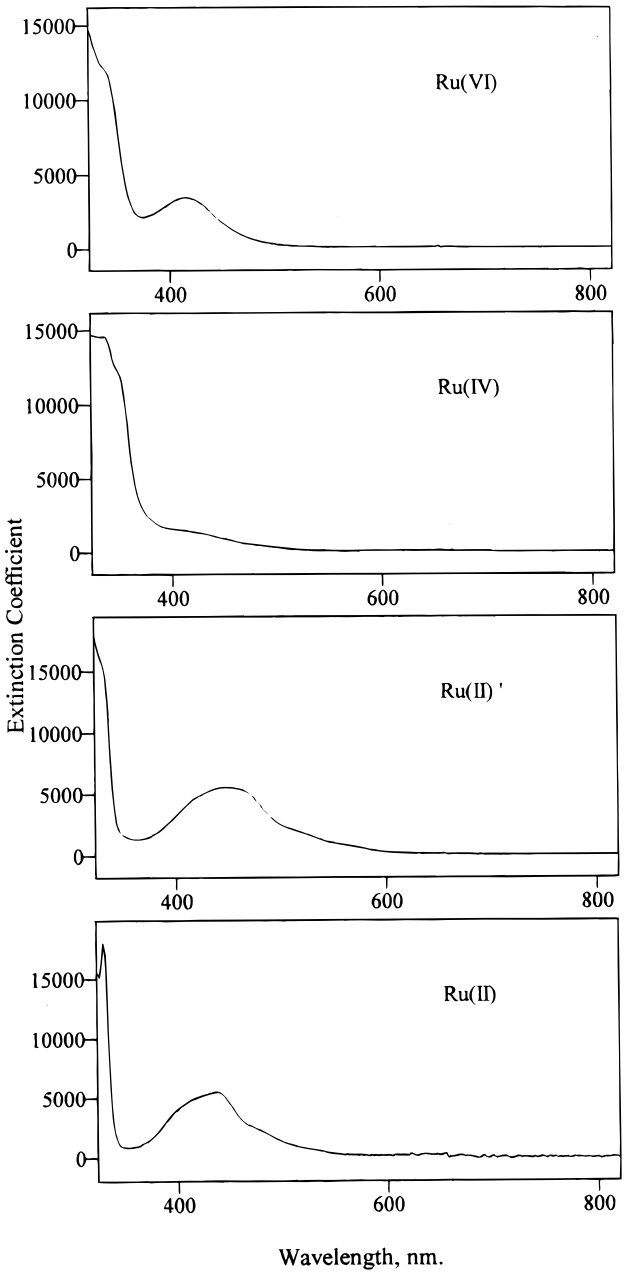

Figure 2. Predicted spectra for *trans*-$[Ru^{VI}(tpy)(O)_2(CH_3CN)]^{2+}$, Ru^{IV}, $Ru^{II'}$, and $[Ru^{II}(tpy)(CH_3CN)_3]^{2+}$ by global analysis of absorbance-time traces in CH_3CN at 25 °C with [Ru^{VI}] initially 1.6×10^{-4} M and benzyl alcohol 1.6×10^{-3} M.

Scheme 1. In Acetonitrile, 25.0 °C

$$trans\text{-}[Ru^{VI}(tpy)(O)_2(CH_3CN)]^{2+} + PhCH_2OH \xrightarrow{k_1} Ru^{IV} + PhCHO \qquad 67(\pm 3)\ M^{-1}\ s^{-1}$$

$$Ru^{IV} + PhCH_2OH \xrightarrow{k_2} Ru^{II'} \qquad 2.4(\pm 0.1)\ M^{-1}\ s^{-1}$$

$$Ru^{II'} + CH_3CN \xrightarrow{k_3} [Ru^{II}(tpy)(CH_3CN)_3]^{2+} + PhCHO \qquad 1.13(\pm 0.06) \times 10^{-4}\ s^{-1}$$

There is no evidence for $[Ru^{III}(tpy)(CH_3CN)_3]^{3+}$ or other Ru^{III} intermediates in the reduction of Ru^{IV} to Ru^{II}. In reactions involving *cis*-$[Ru^{IV}(bpy)_2(py)(O)]^{2+}$, reduction to *cis*-$[Ru^{II}(bpy)_2(py)(H_2O)]^{2+}$ is often followed by rapid comproportionation,[8b]

(35) Binstead, R. A.; Stultz, L. K.; Meyer, T. J. *Inorg. Chem.* **1995**, *34*, 546.

(36) For a complete description of the method of Singular Value Decomposition and the use of SPECFIT, see: Malinowski, E. R. *Factor Analysis in Chemistry*, 2nd ed.; Wiley-Interscience: New York, 1991; ref 9 and references cited therein.

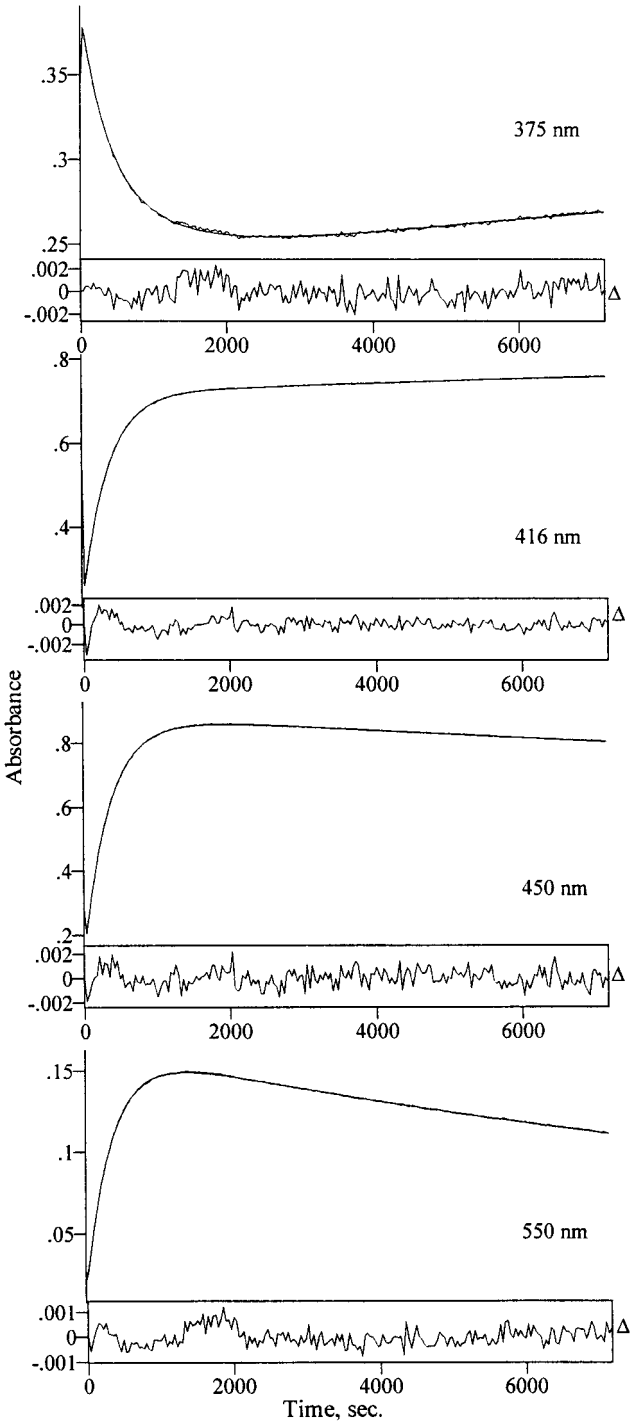

Figure 3. Single wavelength comparisons of experimental and calculated absorbance-time traces and residuals (△) according to Scheme 1 for the reaction between *trans*-$[Ru^{VI}(tpy)(O)_2(CH_3CN)]^{2+}$ (1.6×10^{-4} M) and benzyl alcohol (1.6×10^{-3} M) in CH_3CN at 25 °C.

$$cis\text{-}[Ru^{IV}(bpy)_2(py)(O)]^{2+} + cis\text{-}[Ru^{II}(bpy)_2(py)(H_2O)]^{2+} \rightleftharpoons 2\ cis\text{-}[Ru^{III}(bpy)_2(py)(OH)]^{2+} \quad (11)$$

This complicates the kinetic analysis and introduces Ru^{III} as a secondary oxidant. Analogous reactions between $[Ru^{IV}(tpy)(CH_3CN)_2(O)]^{2+}$ and $Ru^{II'}$ or $[Ru^{II}(tpy)(CH_3CN)_3]^{2+}$ do not occur. The latter reaction is, no doubt, thermodynamically unfavorable since the potential for the $[Ru(tpy)(CH_3CN)_3]^{3+/2+}$ couple is $E_{1/2} = 1.49$ V vs SSCE.[34]

CH_3CN/H_2O Mixtures. Reaction between *trans*-$[Ru^{VI}(tpy)(O)_2(H_2O)]^{2+}$ and $PhCH_2OH$ in acetonitrile 2.85 M in H_2O gives $Ru^{IV}ORu^{IV}$, as the product as shown by UV−visible measurements. One equivalent of benzaldehyde is produced. These observations are consistent with Ru^{VI} reduction to Ru^{IV} followed by rapid dimerization by μ-oxo formation. Under these conditions, the rate constant for $Ru^{VI} \rightarrow Ru^{IV}$ reduction is k (25 °C) $= 28 \pm 4\ M^{-1}\ s^{-1}$ (Table 1).

Discussion

The results presented here establish that the reaction between *trans*-$[Ru^{VI}(tpy)(O)_2(CH_3CN)]^{2+}$ and $PhCH_2OH$ in CH_3CN occurs in three stages: (1) Reduction to Ru^{IV} with the production of PhCHO. (2) Reduction of Ru^{IV} to $Ru^{II'}$. (3) Solvolysis of $Ru^{II'}$ to give $[Ru^{II}(tpy)(CH_3CN)_3]^{2+}$ and PhCHO. These three steps are written out in Scheme 1. In water, Ru^{VI} to Ru^{IV} reduction is followed by rapid dimerization by μ-oxo formation (eq 2). There is more mechanistic insight in CH_3CN, and those results will be discussed first.

Stage 1. $Ru^{VI} \rightarrow Ru^{IV}$. CH_3CN. A number of experimental facts relate directly to the mechanism of Ru^{VI} oxidation of benzyl alcohol. The reaction is first order in both *trans*-$[Ru^{VI}(tpy)(O)_2(CH_3CN)]^{2+}$ and $PhCH_2OH$. The products are Ru^{IV} and PhCHO. Added O_2 has no effect on either the product distribution or the rate constant, suggesting that the redox step involves synchronous or near-synchronous two-electron transfer without formation of intermediate alcohol radicals.[37] There is no evidence for Ru^{V} as an intermediate oxidation state.

Net O atom transfer occurs from Ru^{VI} to $PhCH_2OH$. This is evident from the ^{18}O labeling results which demonstrate that ~50% of the ^{18}O atoms which originate in Ru^{VI} are incorporated in the PhCHO product. It is also consistent with the products of the several mixing studies in CH_3CN which reveal that (1) reduction of *trans*-$[Ru^{VI}(tpy)(O)_2(CH_3CN)]^{2+}$ gives Ru^{IV} but reduction of *trans*-$[Ru^{VI}(tpy)(O)_2(H_2O)]^{2+}$ gives $Ru^{IV}ORu^{IV}$; (2) reduction of *trans*-$[Ru^{VI}(tpy)(O)_2(CH_3CN)]^{2+}$ by hydroquinone, which is known to reduce *cis*-$[Ru^{IV}(bpy)_2(py)(O)]^{2+}$ by proton-coupled electron transfer,[38] also gives $[(tpy)(H_2O)_2Ru^{IV}ORu^{IV}(OH)(H_2O)(tpy)]^{5+}$. The results of these studies suggest that when Ru^{VI} is reduced to Ru^{IV} *and* there is an aqua ligand in the coordination sphere, *e.g.*

$$trans\text{-}[Ru^{VI}(tpy)(O)_2(CH_3CN)]^{2+} + H_2Q \rightarrow [Ru^{IV}(tpy)(O)(H_2O)(CH_3CN)]^{2+} + Q \quad (12)$$

reduction is followed by rapid μ-oxo formation. By inference, μ-oxo formation requires both oxo and aqua groups, and a coupling reaction, probably

$$2\ [Ru^{IV}(tpy)(H_2O)(CH_3CN)(O)]^{2+} \rightarrow [(tpy)(OH)(CH_3CN)Ru^{IV}ORu^{IV}(OH)(CH_3CN)(tpy)]^{4+} + H_2O \quad (13)$$

With *trans*-$[Ru^{VI}(tpy)(O)_2(H_2O)]^{2+}$ as the oxidant in acetonitrile, O-transfer to the alcohol occurs to give $[Ru^{IV}(tpy)(H_2O)(CH_3CN)(O)]^{2+}$ followed by μ-oxo formation. With *trans*-$[Ru^{VI}(tpy)(O)_2(CH_3CN)]^{2+}$, μ-oxo dimer formation does not occur in CH_3CN. By inference, Ru^{IV} does not have a bound water and can be reasonably formulated as $[Ru^{IV}(tpy)(CH_3CN)_2(O)]^{2+}$. This conclusion is also consistent with an O-atom transfer mechanism.

(37) Thompson, M. S.; Meyer, T. J. *J. Am. Chem. Soc.* **1982**, *104*, 4106−4115.
(38) Binstead, R. A.; McGuire, M. E.; Dovletoglou, A.; Seok, W. K.; Roecker, L.; Meyer, T. J. *J. Am. Chem. Soc.* **1992**, *114*, 173−186.

Scheme 2

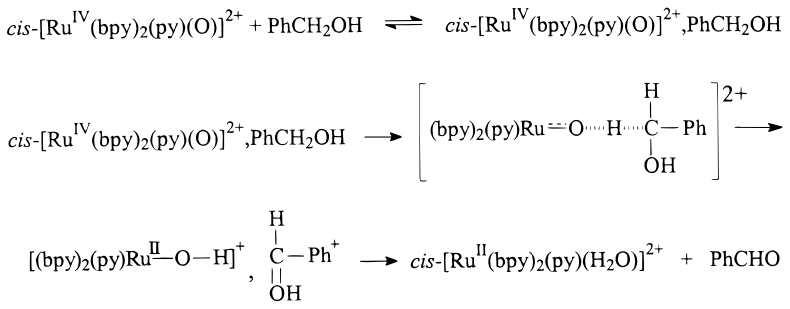

Scheme 3

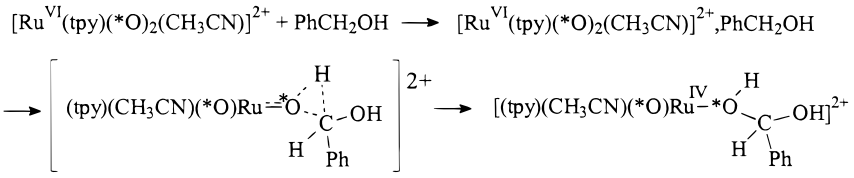

In considering mechanism there is an α,α-CH_2/α,α-CD_2 kinetic isotope effect of $k_H/k_D = 12.1$ at 25 °C for the $Ru^{VI} \rightarrow Ru^{IV}$ reduction . This necessarily implicates C−H bond involvement in the rate-determining step.

The original proposal for oxidation of benzyl alcohol by *cis*-$[Ru^{IV}(bpy)_2(py)(O)]^{2+}$ in water was that the key redox step involved hydride transfer within an association complex of the reactants followed by proton equilibration (Scheme 2). This *cannot* be the mechanism by which Ru^{VI} oxidizes benzyl alcohol in acetonitrile. If it were, $[Ru^{IV}(tpy)(O)(H_2O)(CH_3CN)]^{2+}$ would be an intermediate and $Ru^{IV}ORu^{IV}$ the product by eq 13. A mechanism consistent with the observation of O transfer from the oxo to the $-CH_2-$ C atom is "insertion" into the C−H bond. This mechanism is illustrated in Scheme 3 with the ^{18}O label shown as *O.

The immediate organic product in this case would be a bound aldehyde hydrate. Rapid solvolysis (there is no evidence for an intermediate) would lead to Ru^{IV} and the hydrate

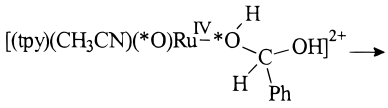

$$[Ru^{IV}(tpy)(CH_3CN)_2(*O)]^{2+} + CH_3CN + PhCH(OH)(*OH) \quad (14)$$

Dehydration cannot occur while the aldehyde is bound to Ru^{IV} because an aqua group in the coordination sphere results in rapid dimerization, which is not observed. Additionally, a satisfactory fit to the data was *not* obtained when the model incorporated dehydration in the coordination sphere. Although a measurable hydration equilibrium exists for the benzaldehyde hydrate in water, it is negligibly small in CH_3CN, eq 15.[39,40] Its release from the coordination sphere followed by dehydration would give free aldehyde and water. Dehydration would explain the experimental observation that ~50% ^{18}O atom transfer occurs, eq 15.

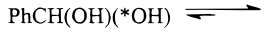

$$½\ PhCHO + ½\ H_2{*}O + ½\ PhCH{*}O + ½\ H_2O \quad (15)$$

No attempt was made to carry out the ^{18}O labeling experiment in water because of O exchange with solvent in the benzaldehyde product through the hydrate.

Cundari and Drago have investigated the relative energies of various reaction pathways in the oxidation of methanol by the hypothetical, stereochemically unencumbered Ru^{IV}═O oxidant *cis*-$[Ru^{IV}(NH{=}CH{-}CH{=}NH)_2(NH_3)(O)]^{2+}$ by applying INDO/1 analysis.[41]

These calculations reveal that the initial Ru═O···H−C interaction in Scheme 2 is attractive, but in the gas phase in the absence of solvent molecules. There is a large barrier to further hydride transfer arising from Ru−O and C−H stretching. For the C−H insertion pathway implied in Scheme 2 the Ru═O/C−H interaction is repulsive at all separation distances and it was concluded that it was unimportant. The lowest energy pathway in their calculations involved coordination expansion with addition of methanol to form the pentagonal plane of a pentagonal bipyramidal intermediate. Coordination activates CH_3OH toward Ru═O insertion into a methanol C−H bond. This mechanism is illustrated schematically for oxidation of $PhCH_2OH$ by Ru^{VI} in Scheme 4. There is a basis for coordination expansion for the d^2 Ru^{VI} dioxo ion given the unoccupied $d\pi$ orbitals. Rather than the dioxo, the seven-coordinate intermediate could be the hydroxy-oxo $[Ru^{VI}(tpy)(O)(OH)(CH_3CN)(PhCH_2OH)]^{2+}$.

For *trans*-$[Ru^{VI}(tpy)(O)_2(CH_3CN)]^{2+}$, prior substitution at a normal coordination site is possible, but only if special nucleophilic properties are ascribed to the alcohol. From earlier studies on H_2O substitution for CH_3CN in CH_3CN, $k_f = 35.3\ M^{-1}\ s^{-1}$ and $k_r = 4.9\ s^{-1}$ for

$$trans\text{-}[Ru^{VI}(tpy)(O)_2(CH_3CN)]^{2+} + H_2O \underset{k_r}{\overset{k_f}{\rightleftharpoons}} trans\text{-}[Ru^{VI}(tpy)(O)_2(H_2O)]^{2+} + CH_3CN \quad (16)$$

Under the same conditions, $k = 67\ M^{-1}\ s^{-1}$ for oxidation of $PhCH_2OH$ showing that oxidation is faster than substitution by water. Rate-limiting substitution also appears unlikely for $PhCH_2OH$ based on the considerable kinetic isotope effect of $k_H/k_D = 12.1$, Table 1. If the true isotope effect is higher and

(39) Bover, W. J.; Auman, P. *J. Chem. Soc., Perkin Trans. 2* **1973**, 786−790.
(40) Greenzaid, P. *J. Org. Chem.* **1973**, *38*, 3164−3167.
(41) Cundari, T. R.; Drago, R. S. *Inorg. Chem.* **1990**, *29*, 3904−3907.

Scheme 4

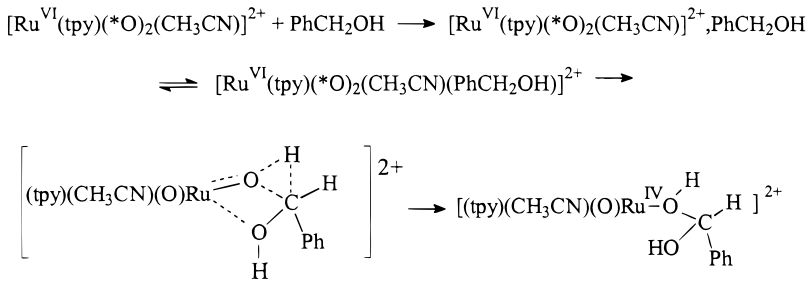

Scheme 5

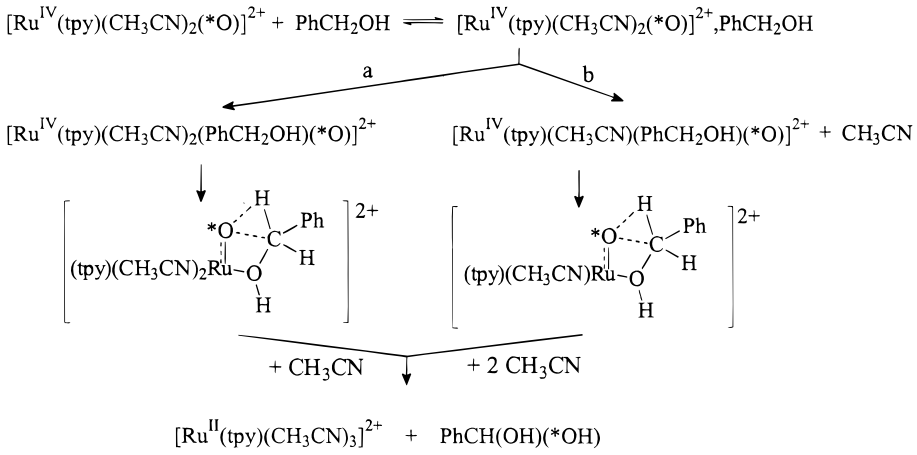

oxidation partly rate limited by substitution, this sets an upper limit for substitution that is far slower than oxidation of $PhCH_2OH$. Competitive substitution and oxidation for $PhCH_2OH$ seem unlikely given the extended linear region found in the Arrhenius plots.

The redox step is characterized by a low activational requirement ($\Delta H^{\ddagger} = 7.5 \pm 0.4$ kcal mol^{-1}) and a large entropy of activation ($\Delta S^{\ddagger} = -33 \pm 2$ eu). The k_H/k_D kinetic isotope effect appears largely in $\Delta H^{\ddagger}$, $\Delta\Delta H^{\ddagger} = \Delta H^{\ddagger}_{D,D} - \Delta H^{\ddagger}_{H,H} = 1.1(\pm 0.1)$ kcal mol^{-1}, revealing an increased activational requirement for the deuterio form.

Stages 2 and 3. $Ru^{IV} \rightarrow Ru^{II'} \rightarrow [Ru^{II}(tpy)(CH_3CN)_3]^{2+}$. CH_3CN. Although we were unable to prepare Ru^{IV} independently, it can be formed in dry CH_3CN with 1 equiv of added $PhCH_2OH$. The available evidence establishes with reasonable certainty that Ru^{IV} is $[Ru^{IV}(tpy)(CH_3CN)_2(O)]^{2+}$. Its rate of oxidation of $PHCH_2OH$ is slower, and kinetically separable from oxidation of $PhCH_2OH$ by *trans*-$[Ru^{VI}(tpy)(O)_2(CH_3CN)]^{2+}$. The rate law is first order in both Ru^{IV} and $PhCH_2OH$.

As for Ru^{VI}, the ^{18}O labeling study demonstrates that net O atom transfer occurs as part of the redox mechanism. In addition, there is clear evidence in the UV−visible and FTIR data for an intermediate that, ultimately, undergoes solvolysis to give PhCHO and $[Ru^{II}(tpy)(CH_3CN)_3]^{2+}$.

There have been other reports of bound intermediates in the oxidation of benzyl alcohol to benzaldehyde by various metal complexes, including a Ru^{V}=O oxidant.[17,42−44] For Ru^{IV} as oxidant, the appearance of MLCT bands characteristic of related Ru^{II}−tpy complexes[27,37] points to oxidation state II as the best oxidation state description for $Ru^{II'}$.

On the basis of the available evidence, oxidation of $PhCH_2OH$ by Ru^{IV} also occurs by O transfer and the intermediate $Ru^{II'}$ is the bound aldehyde hydrate,

$$[Ru^{IV}(tpy)(CH_3CN)_2(O)]^{2+} + PhCH_2OH \rightarrow [Ru^{II}(tpy)(CH_3CN)_2((OH)_2CHPh)]^{2+} \quad (17)$$

Possible structures for $Ru^{II'}$ include the chelate and monodentate forms in **2** and **3**.

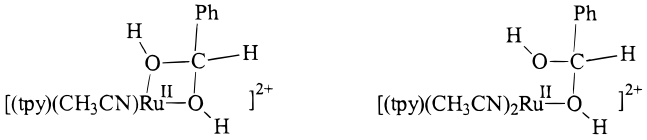

2 **3**

From the time-resolved FTIR data from 1750 to 1300 cm^{-1}, new bands for $Ru^{II'}$ appear at 1479 and 1318 cm^{-1} as well as ν(C=O) at 1702 cm^{-1}. In primary alcohols, the O−H in-plane bend couples with C−H wagging modes to give two bands, typically near 1420 and 1330 cm^{-1}.[45] The bands at 1479 and 1318 cm^{-1} may arise from a combination of these modes or be ν(tpy) modes shifted in the intermediate.

Based on the intervention of O-transfer and the large k_H/k_D kinetic isotope effect there must be significant C−H involvement in the redox step and net C−H insertion. Based on the results of Cundari and Drago, the redox step may be preceded by binding of the alcohol, possibly by coordination sphere expansion as in Scheme 3 for Ru^{VI}. Substitution for CH_3CN in $[Ru^{IV}(tpy)(CH_3CN)_2(O)]^{2+}$ appears to be rapid, and the mechanism in this case could involve prior substitution of $PhCH_2OH$ for CH_3CN in a

(42) Nakao, M.; Nishiyama, S.; Tsuruya, S.; Masai, M. *Inorg. Chem.* **1992**, *31*, 4662−4668.
(43) Banerjee, R.; Das, A.; Dasgupta, S. *J. Chem. Soc., Dalton Trans.* **1990**, 1207−1212.
(44) Sun, W.-Y.; Ueyama, N.; Nakamura, A. *Tetrahedron* **1993**, 1357−1370.
(45) Silverstein, R. M.; Bassler, G. C.; Morrill, T. C. *Spectrophotometric Identification of Organic Compounds*, 5th ed.; John Wiley & Sons, Inc.: New York, 1991; Chapter 3.

Table 2. Rate Constants and Activation Parameters for the Oxidation of Benzyl Alcohol by Ruthenium−Oxo Reagents

oxidant	k (M^{-1} s^{-1})	solvent	$\Delta H^{\ddagger}$ (kcal/mol)	$\Delta S^{\ddagger}$ (eu)
trans-$[Ru^{VI}(tpy)(O)_2(H_2O)]^{2+}$ [a]	13.3	0.1 M $HClO_4$	11.4 ± 0.2	−15.0 ± 1
trans-$[Ru^{VI}(tpy)(O)_2(H_2O)]^{2+}$ [a,d]	1.28	0.1 M $HClO_4$	14.0 ± 0.2	−10.8 ± 1
trans-$[Ru^{VI}(tpy)(O)_2(CH_3CN)]^{2+}$ [a]	67 ± 3	CH_3CN	7.5 ± 0.4	−33 ± 2
trans-$[Ru^{VI}(tpy)(O)_2(CH_3CN)]^{2+}$ [a,d]	5.5 ± 0.3	CH_3CN	8.6 ± 0.4	−34 ± 2
trans-$[Ru^{IV}(tpy)(CH_3CN)_2(O)]^{2+}$ [a]	2.4 ± 0.1	CH_3CN	5.1 ± 0.3	−47 ± 2
trans-$[Ru^{IV}(tpy)(CH_3CN)_2(O)]^{2+}$ [a,d]	0.039 ± 0.002	CH_3CN	9.9 ± 0.5	−39 ± 2
cis-$[Ru^{IV}(bpy)_2(py)(O)]^{2+}$ [b]	2.43 ± 0.03	0.1 M $HClO_4$	5.7 ± 0.2	−38 ± 1
cis-$[Ru^{IV}(bpy)_2(py)(O)]^{2+}$ [b]	0.048	0.1 M $HClO_4$	5.6 ± 0.6	−46 ± 2
$[Ru^{V}(EDTA)(O)]^{-}$ [c,e]	5.2×10^3	pH 5 buffer	4.8	−63
$[Ru^{V}(PDTA)(O)]^{-}$ [c,e]	6.0×10^3	pH 5 buffer	4.7	−64

[a] This work. [b] Reference 23. [c] Kahn, M. M. T.; Merchant, R. R.; Chatterjee, D.; Bhatt, K. N. *J. Mol. Catal.* **1991**, *67*, 309−315. [d] α,α-d_2 benzyl alcohol. [e] EDTA = ethylenediaminetetraacetate anion; PDTA = propylenediaminetetracetate anion.

normal coordination position. If this is the case, the bound alcohol undergoes rapid intramolecular oxidation since there is no evidence for a kinetic intermediate.

Possible mechanisms for Ru^{IV} oxidation of $PhCH_2OH$ involving initial binding to the metal are illustrated in Scheme 5. Again, the ^{18}O label is indicated by the asterisk. The distinction between branches **a** and **b** is in the nature of the substitution, coordination expansion in **a**, and substitution in **b**.

As for Ru^{VI}, release of the hydrate and dehydration would complete the mechanism and explain the observation of ∼50% ^{18}O labeling in the product.

The striking feature about the redox step in this case is the extraordinarily large kinetic isotope effect with k_H/k_D (25 °C) = 61.5. It is even larger than $k_H/k_D = 50$ for *cis*-$[Ru^{IV}(bpy)_2(py)(O)]^{2+}$ as the oxidant in 0.1 M $HClO_4$. These large isotope effects have been discussed elsewhere as a nuclear tunneling phenomenon.[23]

Even though there are similarities in the oxidation of $PhCH_2OH$ by *cis*-$[Ru^{IV}(bpy)_2(py)(O)]^{2+}$ and $[Ru^{IV}(tpy)(CH_3CN)_2(O)]^{2+}$, there are important differences. As shown by the data in Table 2, both have large, negative $\Delta S^{\ddagger}$ values. However for *cis*-$[Ru^{IV}(bpy)_2(py)(O)]^{2+}$ as oxidant, the kinetic isotope effect appears largely as a decrease in $\Delta S^{\ddagger}$, $\Delta\Delta S^{\ddagger} = -8$ eu. For $[Ru^{IV}(tpy)(CH_3CN)_2(O)]^{2+}$, the origin of the isotope effect is in $\Delta H^{\ddagger}$, with $\Delta\Delta H^{\ddagger} = 4.8(\pm 0.3)$ kcal/mol and $\Delta\Delta S^{\ddagger} = +8(\pm 0.4)$ eu. The entropy of activation favors the deuterio substrate. If the mechanisms are the same, this comparison points to the importance of thermal activation to levels above $\upsilon = 0$ for the critical C−H mode in order to enhance vibrational overlap in the tunneling mechanism.

However, detailed comparisons must be made with care. A variety of pathways may be operative in the oxidation of alcohols, including the earlier suggestion of hydride transfer. In the oxidation of 2-propanol to acetone by *cis*-$[Ru^{IV}(bpy)_2(py)(O)]^{2+}$, there is no net O atom transfer as shown by ^{18}O labeling.[23] The key difference between the two Ru^{IV} oxidants could be stereochemical. The tpy-based coordination results in a more open structure at the metal and this may open substitutional pathways that are inaccessible or less facile for the bis-bpy structures.

Ru^{VI} Oxidation in H_2O. There is an increase in rate constant of ∼5 for Ru^{VI} oxidation of $PhCH_2OH$ in CH_3CN compared to 0.1 M $HClO_4$. In H_2O, the reaction remains first order in $PhCH_2OH$ and Ru^{VI}, and PhCHO is the product. The solvent effect between CH_3CN and H_2O is partitioned between bulk solvent and the coordination sphere. This is shown by the rate constant for oxidation of $PhCH_2OH$ by *trans*-$[Ru^{VI}(tpy)(O)_2(H_2O)]^{2+}$ in CH_3CN 2.05 M in H_2O. Under these conditions, $k = 28 \pm 4$ M^{-1} s^{-1}, Table 1, suggesting that the change in inner coordination sphere ligand between CH_3CN and H_2O causes a decrease of ∼2. For the Ru^{VI} reaction in water, there is a very slight H_2O/D_2O kinetic isotope effect with k_{H_2O}/k_{D_2O} (25 °C) = 1.04.

A mechanistic dilemma also exists for Ru^{VI} oxidation in comparing the results in H_2O and CH_3CN as solvents. The kinetics are the same in both and k_H/k_D kinetic isotope effects comparable (at 25 °C), but the patterns of activation parameters between the two solvents are distinctly different. In water, $\Delta\Delta S^{\ddagger} = \Delta S^{\ddagger}_{D,D} - \Delta S^{\ddagger}_{H,H} = +4.2(\pm 0.5)$ eu and $\Delta\Delta H^{\ddagger} = 2.6(\pm 0.1)$ kcal mol^{-1}. In CH_3CN, $\Delta\Delta S^{\ddagger} = -1(\pm 0.5)$ eu and $\Delta\Delta H^{\ddagger} = 1.1(\pm 0.1)$ kcal mol^{-1}. Once again, the implications for mechanism of the change in activation parameters are not understood. In either case, the large k_H/k_D kinetic isotope effect points to the redox step rather than the substitution as rate determining.

Acknowledgment is made to the National Science Foundation under Grant CHE-9503738 for support of this research.

Supporting Information Available: Figure showing absorbance−time traces at various intervals over a period of 2 h for the reaction between *trans*-$[Ru^{VI}(tpy)(O)_2(OH_2)]^{2+}$ (1.21×10^{-4} M) and benzyl alcohol (4.9×10^{-4} M) in 1 M $HClO_4$ at 25.0 °C. IR spectra at various intervals over a 2 h period for the reaction between *trans*-$[Ru^{VI}(tpy)(O)_2(CD_3CN)]^{2+}$ (2.29×10^{-3} M) and benzyl alcohol (2.29×10^{-2} M) in CD_3CN in a 1 mm BaF_2 cell. Plots of k_{obs} versus concentration of benzyl alcohol for the reduction of *trans*-$[Ru^{VI}(tpy)(O)_2(H_2O)]^{2+}$ to $Ru^{IV}ORu^{IV}$ in 0.1 M $HClO_4$ at 25 °C. Plots of $\ln(k/T)$ versus $1/T$ for the oxidation of benzyl alcohol and α,α-d_2 benzyl alcohol by *trans*-$[Ru^{VI}(tpy)(O)_2(H_2O)]^{2+}$ in 0.1 M $HClO_4$. Plots of $\ln(k/T)$ versus $1/T$ for the $Ru^{VI} \rightarrow Ru^{IV}$ stage in the reaction between *trans*-$[Ru^{VI}(tpy)(O)_2(CH_3CN)]^{2+}$ and benzyl alcohol and α,α-d_2 benzyl alcohol, and for the $Ru^{IV} \rightarrow Ru^{II'}$ stage of oxidation for benzyl alcohol and α,α-d_2 benzyl alcohol in CH_3CN. This material is available free of charge via the Internet at http://pubs.acs.org.

IC981040V